

## Ultrafast Conformational Relaxation Dynamics in Anthryl-9-benzothiazole: Dynamic Planarization Driven Delocalization and Protonation Induced Twisting Dynamics

Rajib Ghosh, Amitabha Nandi, Archana Kushwaha, and Dipanwita Das

*J. Phys. Chem. B*, **Just Accepted Manuscript** • DOI: 10.1021/acs.jpcc.9b01373 • Publication Date (Web): 07 Jun 2019

Downloaded from <http://pubs.acs.org> on June 8, 2019

### Just Accepted

“Just Accepted” manuscripts have been peer-reviewed and accepted for publication. They are posted online prior to technical editing, formatting for publication and author proofing. The American Chemical Society provides “Just Accepted” as a service to the research community to expedite the dissemination of scientific material as soon as possible after acceptance. “Just Accepted” manuscripts appear in full in PDF format accompanied by an HTML abstract. “Just Accepted” manuscripts have been fully peer reviewed, but should not be considered the official version of record. They are citable by the Digital Object Identifier (DOI®). “Just Accepted” is an optional service offered to authors. Therefore, the “Just Accepted” Web site may not include all articles that will be published in the journal. After a manuscript is technically edited and formatted, it will be removed from the “Just Accepted” Web site and published as an ASAP article. Note that technical editing may introduce minor changes to the manuscript text and/or graphics which could affect content, and all legal disclaimers and ethical guidelines that apply to the journal pertain. ACS cannot be held responsible for errors or consequences arising from the use of information contained in these “Just Accepted” manuscripts.

# Ultrafast Conformational Relaxation Dynamics in Anthryl-9-benzothiazole: Dynamic Planarization Driven Delocalization and Protonation Induced Twisting Dynamics

Rajib Ghosh<sup>\*†</sup>, Amitabha Nandi<sup>†</sup>, Archana Kushwaha<sup>‡</sup>, Dipanwita Das<sup>‡</sup>

<sup>†</sup>*Radiation and Photochemistry Division, Bhabha Atomic Research Centre, Mumbai 400085, India,*

<sup>‡</sup>*Department of Chemistry, Institute of Chemical Technology, Nathalal Parekh Marg, Matunga, Mumbai 400019, India,*

## Abstract

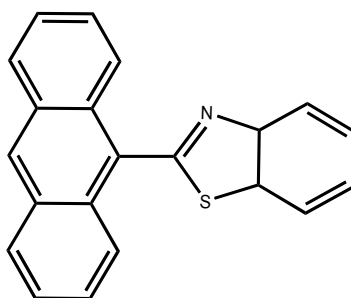
Conformational motion in the excited state of fluorophores critically governs their photophysical properties. Unveiling controlling parameters of photoinduced molecular motion in organic dyes is essential for optimization of light triggered processes. Herein, we present ultrafast dynamics of conformational relaxation controlled photophysical properties of anthryl-9-benzothiazole (AnBT). The title compound is a bichromophore, consists of anthracene (AN) and benzothiazole (BT) units connected by a single bond and exists in out of plane ground state conformation (dihedral angle of about 65°). Vibronic resolved structured absorption feature of anthracene localized excitation is lost in first excited singlet state displaying large Stokes shifted fluorescence, characteristics of delocalized state involving both AN and BT unit. Ultrafast transient absorption spectroscopic studies revealed evolution of anthracene localized Franck-Condon state to a delocalized excited state in a few picosecond timescale depending on solvent viscosity. A planarized motion of AN and BT units is proposed to be involved in excited state relaxation. However, protonation of BT unit is shown to induce significant intramolecular charge transfer facilitated by ultrafast torsional relaxation promoting nonradiative deactivation. Thus, depending upon protonation state, AnBT is shown to undergo either ultrafast planarized motion facilitating delocalized emissive excited state or perpendicular torsion rendering nonemissive twisted intramolecular charge transfer (TICT) state. Experimental results were corroborated by quantum chemical calculation.

## 1. Introduction

Conformational relaxation in excited electronic states of organic dyes governs photophysical properties and plays pivotal role in photonic, optoelectronic and solar energy harvesting application.<sup>1-12</sup> Real time capture of dynamical events associated to geometrical relaxation in photoinduced excited state of organic light absorbing chromophores provides molecular level insight to structure-property relation in chemical dynamics of potential application related to photovoltaics, nonlinear optics, as well as fundamental electron and charge transfer processes in chemistry and biology. Localization and delocalization of excitation energy induced by structural motion in excited state is implicated in solar energy harvesting efficiencies in polymers<sup>11-15</sup>, organic dyes<sup>1,4</sup> and inorganic complexes.<sup>5,6</sup> Dynamic planarization of the different segment of a polymer in the excited state has been revealed to be linked to charge transfer characteristics which has been shown to directly influence solar conversion efficiency.<sup>11</sup> Excited state geometric planarization of ligand substituents and / bridging ligands in ruthenium complexes is shown to decisively impact on charge separation and charge recombination dynamics with major consequence to dye sensitized solar cell efficiency.<sup>5, 6</sup> Exciton delocalization in tailor-made oligomers of phenylene, thiophene, porphyrin, etc., is shown to be facilitated by excited state planarization of individual chromophores as well as bridging linkers.<sup>10, 16-19</sup> On the other hand, photoinduced torsion of intramolecularly connected segments of molecular fluorophores has long been subject of intense investigation in connection to fundamental understanding of twisted intramolecular charge transfer (TICT) as well as prospective application in different photonic and sensing applications.<sup>20, 21</sup> In particular, excited state torsion induced nonradiative deactivation in molecules, popularly classified as ‘molecular rotor’ is projected to have widespread practical application in microscopic sensing and imaging of wide varieties of complex chemical and biological environments.<sup>22-25</sup> In essence, unraveling factors governing molecular motion in excited state is of great significance for fundamental photoinduced chemical dynamics and applied aspects of light driven molecular devices.

Thorough understanding of influence of ultrafast excited state geometric motion on delocalization/localization of electronic energy and electronic charge distribution require probing of simpler molecular system with sufficient temporal resolution. Aiming at molecular level understanding of conformational relaxation guided photophysical properties in organic dyes; herein we present photophysics and excited state structural relaxation dynamics of anthryl-9-benzothiazole (AnBT, refer to Figure 1 for molecular structure) using steady state and time resolved optical spectroscopic methods. Choice of AnBT as the probe serves several

1  
2 purposes. Firstly, the molecule consists of directly linked two planar segments, namely  
3 anthracene (AN) and benzothiazole (BT), has only one conformational degree of freedom and  
4 hence, time resolved optical spectroscopic signatures may be easily correlated to light triggered  
5 dynamical geometry evolution. Secondly, BT group could easily be protonated by adding acid  
6 externally<sup>26, 27</sup>, opening up the opportunity to probe effect of induced charge transfer on  
7 conformational relaxation dynamics. In addition, benzothiazole functionalized donor-acceptor  
8 organic dyes find practical application in two photon absorption<sup>28, 29</sup>, dye sensitized solar cell<sup>30-</sup>  
9 <sup>31</sup> and memory devices<sup>32</sup> and hence in-depth understanding of excited state relaxation dynamics  
10 of benzothiazole based chromophores is desired to provide design input to efficiency  
11 optimization in proposed applications. Given the wider implication of conformational  
12 relaxation in optoelectronic application of organic chromophores in general and practical  
13 application of benzothiazole dyes in particular, herein we present ultrafast dynamics of neutral  
14 and protonated AnBT by femtosecond resolved transient visible pump- visible probe  
15 spectroscopy. We show that excited state conformational relaxation in ultrafast timescale  
16 controls photophysical properties of the dye and direction of rotation is possible to tune by  
17 protonation. Implication of ultrafast torsion guided photophysical properties of neutral and  
18 protonated AnBT is discussed.



31  
32  
33  
34  
35  
36  
37  
38  
39  
40  
41  
42  
43 **Figure 1:** Molecular Structure of Anthryl-9-benzothiazole (AnBT).

## 44 45 **2. Experimental Section**

46  
47 AnBT was synthesized by condensation of 9-anthraldehyde and 2-aminothiophenol by  
48 microwave method. Briefly, 9-anthraldehyde (3 mmol) and 2-aminothiophenol (3mmol) in 1:1  
49 molar proportion were dissolved in dry and distilled dichloromethane followed by addition of  
50 silica (3g). The slurry was dried under reduced pressure and irradiated under microwave at  
51 600W for 10 min. The product was extracted with diethylether and concentrated under  
52 vacuum, purified by column chromatography (5% ethyl acetate : ether) and characterized by  
53 proton NMR spectroscopy(<sup>1</sup>H-NMR  $\delta$  (400 MHz, CDCl<sub>3</sub>): 8.62 (s, 1H), 8.25 (dd, J =8.1, 0.5  
54 Hz, 1H), 8.04 (dd, J =13.4, 4.8 Hz, 3H) 7.84-7.79 (m, 2H), 7.64-7.59 (m, 1H), 7.54 (dd, J =8.0,

1  
2 1.1 Hz, 1H), 7.51-7.41 (m, 4H). Solvents used for optical experiments were of spectroscopic  
3 grade (Spectrochem India) and all spectroscopic experiments were carried out at 295 K. Sample  
4 was dissolved in different solvents and concentration was adjusted to maintain absorbance of  
5 about 0.1 in 1 cm cuvette for steady state measurements and about 0.2 in 1 mm cuvette for  
6 ultrafast transient absorption and fluorescence upconversion experiments. For spectroscopic  
7 studies of protonated AnBT, protonation was achieved by adding hydrochloric acid diluted in  
8 desired solvents. Shift in absorption spectrum and decrease in emission spectrum was  
9 monitored during addition of hydrochloric acid. The saturation in absorption and emission  
10 spectrum were considered as completion of protonation step.  
11  
12  
13  
14  
15  
16  
17

18  
19 Steady state optical measurements were recorded by JASCO absorption spectrometer  
20 (V670) and Horiba-Jobin-Yvon (Fluorolog-3) spectrofluorimeter. Fluorescence spectra were  
21 corrected for wavelength dependent instrument sensitivity. Nanosecond time resolved emission  
22 spectroscopic measurements were conducted by time correlated single photon counting  
23 technique (TCSPSC, Edinburgh, IBH). To resolve ultrafast emission decay kinetics,  
24 fluorescence upconversion technique (FOG, CDP Corporation, Russia) was employed.  
25 Ultrafast excited state dynamics were resolved using visible-pump visible-probe transient  
26 absorption spectroscopic set up (from CDP corporation, Russia) coupled with a femtosecond  
27 amplified laser system from Amplitude Technologies, France, as described previously.<sup>33</sup>  
28 Briefly, samples were excited with 100 fs laser pulses at 390 nm and transient spectra in entire  
29 visible wavelengths were recorded using femtosecond white light continuum as probe pulse at  
30 different time delays of pump and probe pulse. Sample solution of 1 mm thickness (absorbance  
31 ~0.2 at 390 nm) was rotated during femtosecond measurements. Polarization of pump and  
32 probe beam were kept at magic angle to avoid any temporal dynamics associated to  
33 depolarization dynamics. The transient spectra were corrected for the temporal chirp of probe  
34 wavelengths. The transient kinetics at different wavelengths were fitted with sum of  
35 exponentials convoluted with Gaussian instrument response function of 150 fs. Following  
36 sequential model, global analysis of the TA data was performed to verify the time constants  
37 obtained from selected wavelength kinetic fit. Global analysis was carried out using an open-  
38 source program OPTIMUS developed by Slavov et. al.<sup>34</sup>  
39  
40  
41  
42  
43  
44  
45  
46  
47  
48  
49  
50  
51  
52  
53

54 Quantum chemical calculations were performed by DFT and TDDFT method using GAMESS  
55 software package.<sup>35</sup> B3LYP functional and 6-311G (d, p) basis set were employed along with  
56 polarizable continuum model to incorporate solvent polarity effect. Ground state structure was  
57 optimized without any symmetry restriction. Then vertical excitation energies were calculated  
58 at different torsion angle between AN and BT units keeping all other internal coordinates rigid.  
59  
60

Then, geometry optimization in the  $S_1$  state was performed starting with minimum energy conformation obtained from rigid potential energy scan, however, without any constraint. Further,  $S_1$  to  $S_0$  transition energies were calculated for the excited state optimized geometry.

### 3. Results and Discussion

Steric hindrance between relatively larger sulphur atom of BT with adjacent hydrogen of AN, the two segments in AnBT exist largely in out of plane conformation, with a dihedral angle of about  $65^\circ$  in ground state equilibrium (*see below for quantum chemical calculation*). Large dihedral angle does not allow effective electronic interaction between AN and BT units. Consequently, absorption spectrum of AnBT exhibits vibronic structures typical of anthracene excitation. Interestingly, unlike anthracene, steady state emission of AnBT is largely Stokes shifted and vibrational features are completely lost indicating involvement of BT moiety in excited electronic state (Figure S1, SI). We note that absorption and fluorescence spectra of AnBT presented here perfectly matches with reported literature.<sup>36</sup> As spectral feature of anthracene localized absorption is lost in emission spectrum, we infer that evolution of electronic structure from locally excited (LE) state to a delocalized state in  $S_1$  potential energy surface of AnBT

is possibly guided by geometric relaxation. However, distributions of conformations with different dihedral angles between AN and BT units may also contribute to broadening and loss of structure in emission band. To unravel the structural relaxation induced electronic delocalization, femtosecond pump-probe transient absorption spectroscopic measurements were carried out.

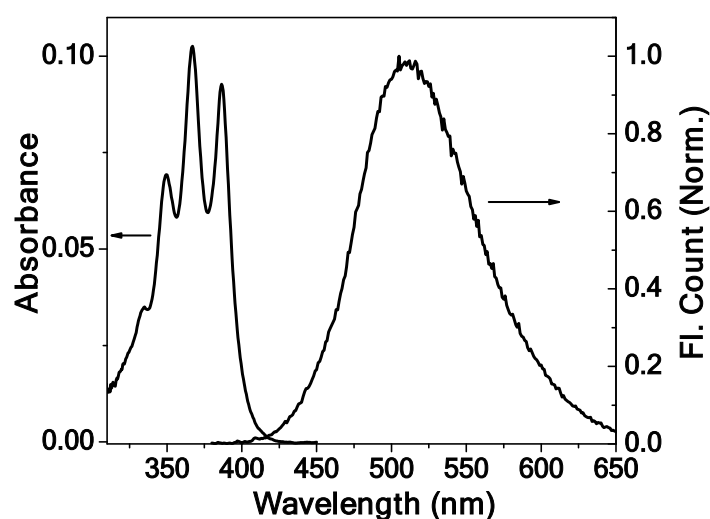


**Figure2:** Steady state absorption and fluorescence spectra of AnBT in acetonitrile.

1  
2  
3  
4  
5  
6  
7  
8  
9  
10  
11  
12  
13  
14  
15  
16  
17  
18  
19  
20  
21  
22  
23  
24  
25  
26  
27  
28  
29  
30  
31  
32  
33  
34  
35  
36  
37  
38  
39  
40  
41  
42  
43  
44  
45  
46  
47  
48  
49  
50  
51  
52  
53  
54  
55  
56  
57  
58  
59  
60

Figure 3A displays transient absorption (TA) spectral evolution of AnBT in acetonitrile following excitation by a 100 femtosecond laser pulse at 390 nm. Differential absorption at 100 fs is characterized by a structured negative band at 430 nm and a narrow excited state absorption (ESA) band located at 590 nm. The structured negative absorption band corresponds to stimulated emission (SE) of anthracene localized excited state and the positive band is attributed to anthracene ESA band.<sup>37</sup> The structured SE band quickly evolves to a red shifted structure-less signal and ESA band at 590 nm concomitantly undergoes significant blue shift to 560 nm in early 600 fs. On further time delay, SE band in 450 nm region evolves to ESA signal, while ESA in red region decays to appear as weak SE signal at 570 nm. At 5 ps delay, differential absorption spectrum is characterized by an ESA peak at 450 nm and a weak SE signal at 570 nm, which does not evolve over several hundreds of picosecond in agreement to long fluorescence lifetime of relaxed  $S_1$  state of AnBT (Figure S2, SI). We infer that structural and electronic relaxation of AnBT in  $S_1$  manifold is accomplished within 5 ps timescale. The early time spectral evolution suggests that LE state reached upon 390 nm excitation relaxes in biphasic manner. Initial ultrafast relaxation is achieved in first few hundred femtosecond followed by picosecond relaxation to the equilibrium geometry in the  $S_1$  potential energy surface. Indeed, short time temporal kinetics at different selected wavelengths fit biexponentially with time constants of about 200 fs and 1.5 ps (Figure 3B). Global analysis of the transient spectral data (Figure S3 in SI) also confirms that excited state evolution of AnBT is associated with two dynamic relaxation processes with average time constant of about 0.17 ps and 1.32 ps. Ultrafast relaxation component ( $\tau \sim 180$  fs) associated to loss of anthracene LE character may be driven by intramolecular structural relaxation which allows mixing of orbital of AN and BT in  $S_1$  surface.<sup>38</sup> Subsequent diffusional motion of AN and BT units towards planarized geometry results in delocalization of excitation energy in picosecond timescale.<sup>39-41</sup> The ultrafast component may also have contribution from dynamical inertial motion of polar solvent molecules which could facilitate charge transfer between two segments leading to loss of LE character.<sup>42</sup>

To confirm or rule out involvement of solvation dynamics in ultrafast relaxation of AnBT, we compared TA dynamics in nonpolar solvent, such as cyclohexane and moderate polarity solvent such as ethyl acetate (Figure S4 and S5 in SI). We note that transient spectral evolution in cyclohexane and ethyl acetate is almost identical to that in acetonitrile. The biphasic relaxation in cyclohexane occurs with lifetime of 260 ( $\pm 20$ ) fs and 3.1 ( $\pm 0.1$ ) ps, while the same accomplishes in ethyl acetate with time constant of 210 ( $\pm 20$ ) fs and 1.9 ( $\pm 0.1$ ) ps (Figure S4). The lifetime of ultrafast component is very close in nonpolar cyclohexane,

medium polar ethyl acetate and polar acetonitrile. Hence influence of solvent relaxation on ultrafast relaxation of AnBT seems to play minor role. We tentatively propose that intramolecular structural reorganization (without large amplitude conformational change) possibly induces electronic delocalization followed by slow diffusional relaxation of AN and BT segments to attain excited state equilibrium geometry. Absence of solvent polarity effect on the excited state relaxation dynamics may possibly due to lower degree of photoinduced charge transfer upon  $S_0$  to  $S_1$  transition as supported by weak solvatochromism of emission maximum from nonpolar to polar solvents (Figure S6A in SI). Quantitative measurement of solvatochromic Stokes shift as a function of solvent polarity parameter (Lippert-Mataga analysis) suggests change in dipole moment upon  $S_1 \leftarrow S_0$  transition is only about 2.8 Debye (Figure S6B in SI). Weak charge transfer character of AnBT in  $S_1$  state does not effectively couple solvent polarization and thus experiences negligible influence from solvent polarity during excited state relaxation. However, the second component is significantly longer in cyclohexane than that in acetonitrile. Higher viscosity of cyclohexane possibly slows down the diffusive conformational planarization dynamics.

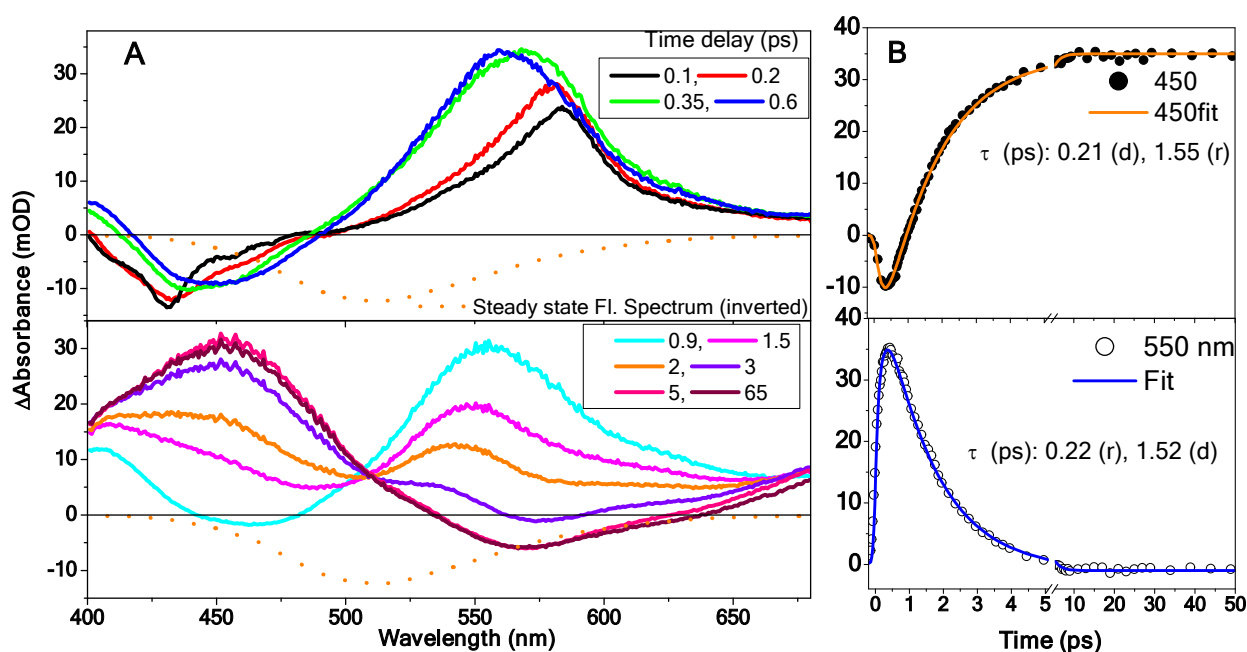


**Figure 3:** (A) Transient spectral evolution of AnBT in acetonitrile following 390 nm femtosecond laser excitation. (B) Temporal dynamics of transient absorption signal at two selected wavelengths. Instrument response convoluted biexponential fit (solid line) and associated time constants (in picosecond) are also indicated in inset. Note that long lived nanosecond component is not shown.

To get further insight about the nature of motion in the excited relaxation processes of AnBT, we measured TA dynamics in solvents of varying viscosities presented in Figure 4 and summarized in Table 1. We note that in all solvents, relaxation dynamics of AnBT is biphasic with an ultrafast component ( $\tau_1$  in the range of 220 - 270 fs) and a slower picosecond

component ( $\tau_2$ ) which systematically varies with solvent viscosity (Table 1). Plot of  $\tau_2$  against solvent viscosity shows a linear variation (Figure 5). Diffusional segmental motion in molecular chromophore is known to be hindered by surrounding viscous friction offered by solvents environment<sup>39-41</sup> and previous studies have well established viscosity dependence of ultrafast dynamics in molecules involving conformation relaxation.<sup>39-41, 43-45</sup> A linear correlation of picosecond relaxation timescale with solvent viscosity is in clear consonance with conformational motion of AN and BT units to attain equilibrium geometry in  $S_1$  surface.

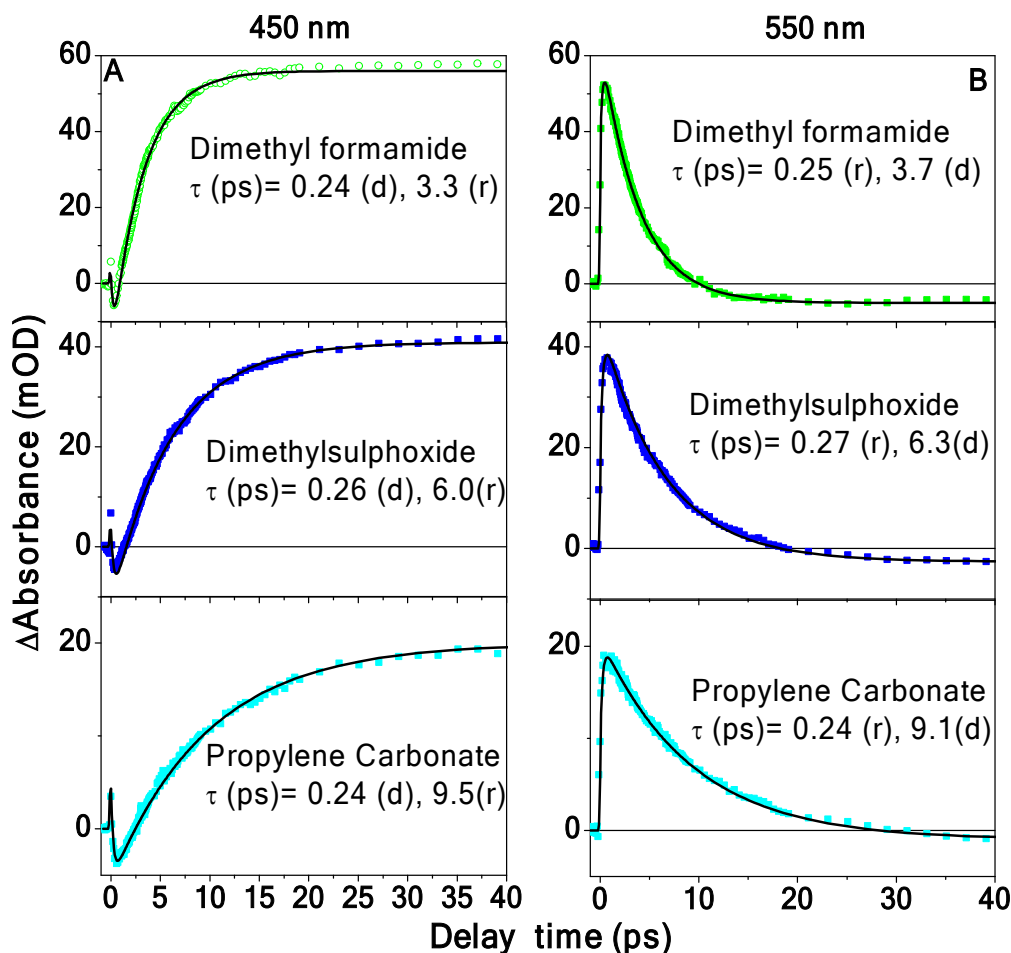


**Figure 4:** Transient absorption dynamics of AnBT at two selected wavelengths (A) 450 nm and (B) 550 nm in dimethylformamide, dimethylsulfoxide and propylene carbonate. Ultrafast time constants associated with best fit function (black solid line) are indicated (also provided in Table 1). Note that nanosecond long component is not indicated.

**Table 1:** Ultrafast Time constants associated with transient absorption dynamics of AnBT in different aprotic solvents of varying viscosities.

Solvent	Viscosity (cp) <sup>a</sup>	Time constant (ps)	
		$\tau_1$	$\tau_2$
Acetonitrile	0.37	0.22	1.5
Ethyl Acetate	0.46	0.22	1.9

Dimethyl Formamide	0.88	0.24	3.3
Cyclohexane	0.9	0.24	3.2
Dimethyl Sulfoxide	1.9	0.26	6.1
Propylene Carbonate	2.6	0.24	9.4

<sup>a</sup>Viscosity (in centipoise) of the solvents taken from Ref. 46.

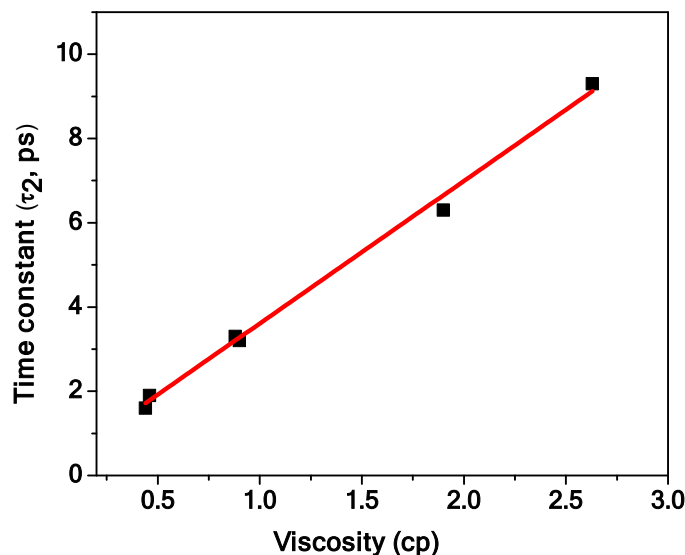
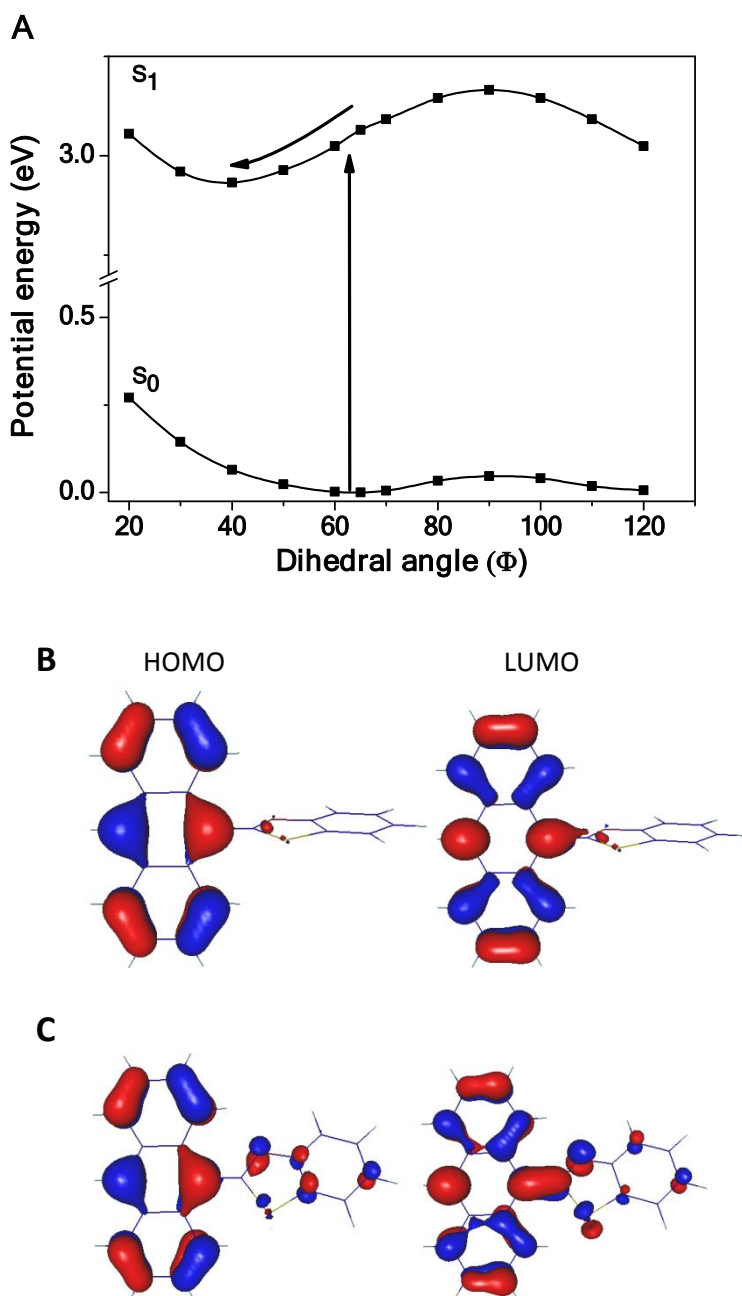


**Figure 5:** Linear variation of  $\tau_2$  of AnBT versus solvent viscosity (Slope = 0.96) as measured in cyclohexane, ethyl acetate, acetonitrile, dimethylformamide, dimethylsulfoxide and propylene carbonate.

To support our proposition of dynamic planarization induced excited state delocalization, we carried out quantum chemical calculation in ground and excited electronic state of AnBT (Figure 6). DFT optimized geometry in ground electronic state of AnBT suggests, at energy minimized conformation AN and BT units exist at a dihedral angle of about  $65^\circ$ . Molecular orbital compositions, shown in Figure 6B, reveals that both HOMO and LUMO orbitals are localized in anthracene units indicating minimal electronic interaction between AN and BT units, which is in complete corroboration with experimentally observed anthracene like absorption spectrum. Then we calculated potential energies (PE) of both  $S_0$  and  $S_1$  state of AnBT as a function of dihedral angle between AN and BT units (Figure 6A). In ground state, increase or decrease in dihedral angle away from equilibrium conformation increases potential energy. However, in  $S_1$  state, PE decrease, as we decrease the dihedral angle and reaches minimum at a dihedral angle of about  $35^\circ$ . Further decrease in dihedral angle results in increase in PE, possibly due to overriding steric repulsion at closer proximity of bulky sulphur of BT with adjacent hydrogen atom of AN. Orbital composition at planarized ( $\Phi \sim 35^\circ$ ) conformation shows that HOMO and LUMO electron density is distributed on both AN and BT units (Figure 6C) which supports delocalized electronic state promoted by planarization of AnBT in  $S_1$

1  
2 surface, consistent with picosecond dynamics measured experimentally. We note that further  
3 planarization ( $\Phi < 35^\circ$ ) would enhance electronic delocalization but energetically unfavorable  
4 due the overwhelming steric repulsion toward coplanar geometry. There is a compromise  
5 between dynamic planarization facilitated electron delocalization induced stabilization and  
6 destabilization by steric repulsion.  
7  
8  
9



53  
54  
55  
56  
57  
58  
59  
60

**Figure 6:** (A) Potential energies of AnBT in  $S_0$  and  $S_1$  state as a function of dihedral angle between AN and BT units (rigid scan, i.e., all other internal coordinates were kept fixed). HOMO-LUMO composition of AnBT in ground state (B) and excited state (C) equilibrium geometry. Calculations were performed employing B3LYP functional and 6-31G(d,p) basis set in acetonitrile (polarizable continuum model).

1  
2  
3  
4  
5  
6  
7  
8  
9  
10  
11  
12  
13  
14  
15  
16  
17  
18  
19  
20  
21  
22  
23  
24  
25  
26  
27  
28  
29  
30  
31  
32  
33  
34  
35  
36  
37  
38  
39  
40  
41  
42  
43  
44  
45  
46  
47  
48  
49  
50  
51  
52  
53  
54  
55  
56  
57  
58  
59  
60

Geometry optimization in  $S_1$  state confirms planarized conformation and  $S_0 \leftarrow S_1$  transition energy is calculated to be about 2.63 eV as compared to 3.38 eV for  $S_0 \rightarrow S_1$  transition at ground state geometry. The calculated Stokes shift (0.75 eV) reasonably agrees with experimental value of 0.93 eV measured in acetonitrile (see Fig. 2). Hence, in conjunction with quantum chemical calculation and steady state photophysical data, ultrafast transient spectroscopic investigation revealed dynamic planarization induced excitation delocalization in AnBT bichromophoric system. Our result is in corroboration with proposed dynamic structural motion induced exciton delocalization reported for various oligomer and polymers.<sup>8-12</sup>

In following section, we present the effect of protonation of benzothiazole unit on photophysics and excited state dynamics of AnBT. Protonation of benzothiazole derivatives and related molecular systems is known to impart intramolecular charge transfer (ICT) character in excited electronic state.<sup>47-49</sup> Torsional relaxation in excited state of ICT molecules is a well documented fundamental phenomena in chemical physics and bears relevance in many practical applications.<sup>20,21</sup> Protonation activated geometrical relaxation is also projected to be important in molecular switch<sup>50,51</sup>, molecular motor<sup>52</sup> and molecular rotor<sup>53,54</sup> applications. As presented below, we show that protonation alters the excited state relaxation dynamics in AnBT and consequently photophysical properties get significantly modulated.

Effect of protonation on steady state absorption and fluorescence spectrum of AnBT is shown in figure 7. Protonation induces red shift of absorption spectrum and the vibrational feature of anthracene localized excitation is largely smeared out which suggest a low energy charge transfer excitation is switched on by protonation. Steady state emission gets quenched over several hundred folds suggesting fast nonradiative relaxation promoted by protonation. Fast nonradiative deactivation of protonated AnBT is corroborated from ultrafast time resolved emission study (Inset of Figure 7), which shows emission lifetime of protonated AnBT is only about 5 picosecond, as compared to nanosecond lifetime (*ca.* 5.4 ns) of neutral AnBT.

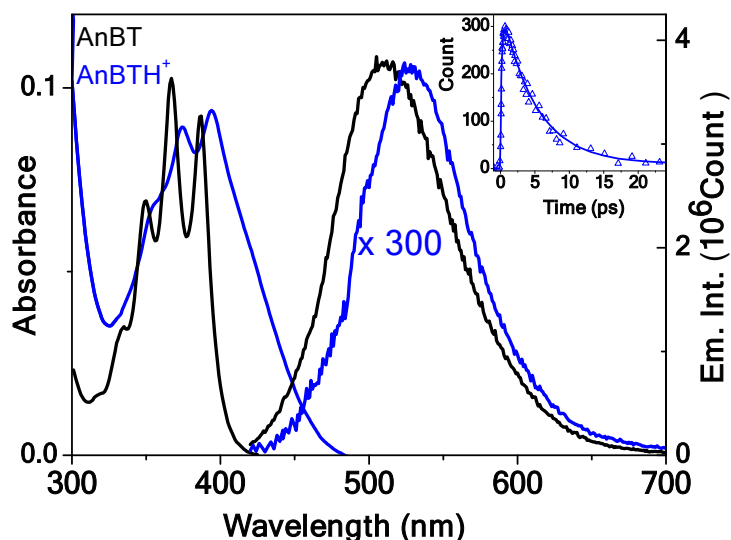


**Figure 7:** Steady state absorption and fluorescence spectra of neutral and protonated AnBT in acetonitrile. Emission spectra were collected at 390 nm excitation. Inset: Transient emission decay kinetics of protonated AnBT in acetonitrile measured by fluorescence upconversion technique ( $\lambda_{\text{ex}} = 390 \text{ nm}$ ,  $\lambda_{\text{em}} = 550 \text{ nm}$ ).

Fast nonradiative deactivation of AnBT upon protonation is attributed to activation of an ultrafast torsional relaxation channel. To identify, ultrafast TA measurements were carried out on protonated AnBTH<sup>+</sup> in acetonitrile. As presented in figure 8A, early time TA spectrum exhibits a weak structured SE band at 460 nm and a weak broad ESA in red region. ESA in 650 nm and higher wavelengths may be assigned to anthracene radical cation absorption due to charge transfer excitation in AnBTH<sup>+</sup> leads to electron transfer from anthracene to BT unit. The weak SE evolves to a strong ESA band with peak at 490 nm and ESA at 550 nm region decays to appear as weak SE band in first few hundred femtosecond. ESA at 550 nm may be assigned to absorption of BT radical as previously observed in TA spectral dynamics of thioflavin-T.<sup>43</sup> This initial spectral evolution is qualitatively similar to that of neutral AnBT and tentatively assigned to planarized motion induced excited state delocalization. Interestingly, with further time delay, SE band decays completely and at 15 ps, TA spectrum appears as broad ESA band covering entire spectral region. This is in contrast to ultrafast planarization dynamics of neutral AnBT, which leads to long lived emissive state. In protonated AnBT, decay of SE within 15 ps suggests relaxation of emissive state to a dark intermediate state. The dark excited state decays back to ground electronic state in 100 ps time scale. Apparently, excited state relaxation dynamics of AnBT changes dramatically on protonation. While, initial TA spectral evolution may have contribution from solvent relaxation dynamics of intramolecular charge transfer state of AnBTH<sup>+</sup>, subsequent nonradiative deactivation channel in protonated AnBT is promoted by formation dark intermediate state which further decays to ground state within 100 ps timescale. The temporal kinetics fit three exponentially

with lifetime of about  $0.23 (\pm 0.03)$ ,  $5 (\pm 1)$  and  $28 (\pm 2)$  ps (Figure 8B). Global analysis of the temporal dynamics of TA signal in entire probe wavelength region yields similar time constants of the three processes (Figure S7 in SI). The ultrafast component may be attributed to solvation dynamics. However, we also note that 390 nm laser, excites AnBTH<sup>+</sup> to S<sub>1</sub> state with significant vibrational energy and thus ultrafast component may have contribution of vibrational relaxation component. The second component of 5 ps associated to decay of emissive planarized state to an intermediate dark state is further characterized by ultrafast emission decay measurement carried out by fluorescence upconversion technique. Transient emission decay lifetime of AnBTH<sup>+</sup> is determined to be 5 ps, in perfect agreement to the time constant measured by TA study. Intermediate dark state decays back to ground state with a lifetime of about  $28 (\pm 2)$  ps. Short lifetime of the S<sub>1</sub> state of AnBTH<sup>+</sup> can be attributed to small energy gap between S<sub>0</sub> and S<sub>1</sub> state. Intermediate dark state is proposed to be formed by mutual torsion of AN and BT units to a twisted structure. Involvement of large amplitude torsion associated to intermediate relaxation component of AnBTH<sup>+</sup> gains support from viscosity dependence study (Figure S8 in SI) which display significant slow-down ( $\tau_2 = 16 (\pm 2)$  ps) of intermediate process in higher viscosity propylene carbonate ( $\eta = 2.6$ ) as compared to that in acetonitrile ( $\eta = 0.4$ )

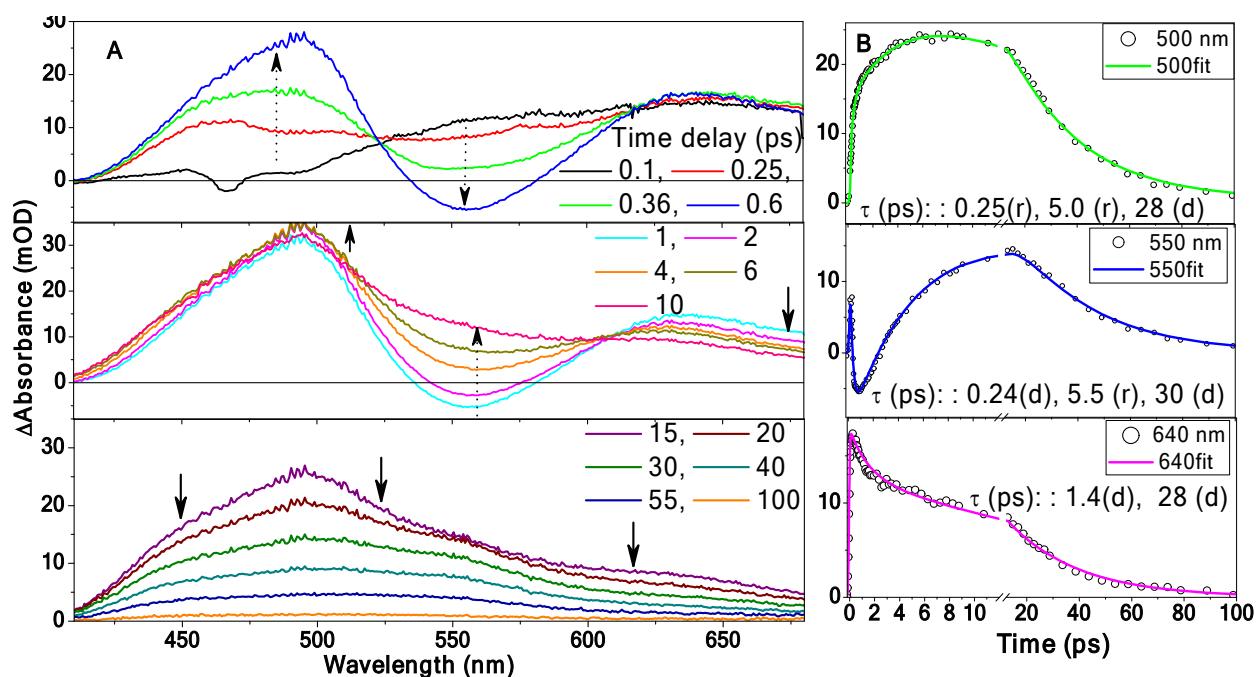


**Figure 8:** (A) Transient spectral evolution of protonated AnBT in acetonitrile, following 390 nm femtosecond laser excitation. (B) Temporal dynamics of TA signal at two selected wavelengths. Instrument response convoluted sum of exponential fit (solid line) and associated time constants (in picosecond) are also shown.

Quantum chemical calculations were carried out to provide further support to the experimental observation (Figure 9). DFT calculated ground state geometry shows that ground state conformation of AnBT remains same upon protonation, as protonation seems to impart

no extra steric influence on already pretwisted conformation of AnBT. However, HOMO-LUMO composition (Figure 8B) indicates charge transfer from AN to BT. This is in contrast to completely AN localized Franck-Condon excited state of neutral AnBT. Protonation is proposed to significantly increase electron pulling capacity of BT enabling CT character in the lowest energy electronic transition manifesting broad shoulder in red side of absorption band along with loss of vibrational structure of pure anthracene like absorption of AnBT.

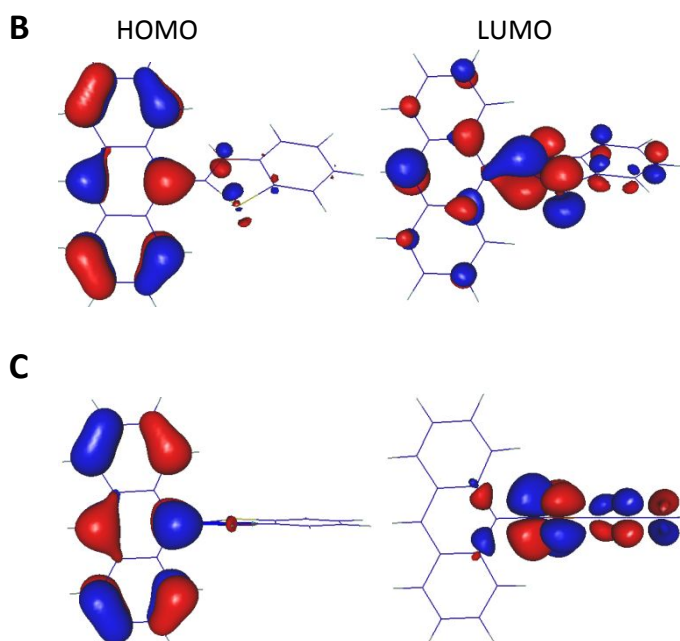
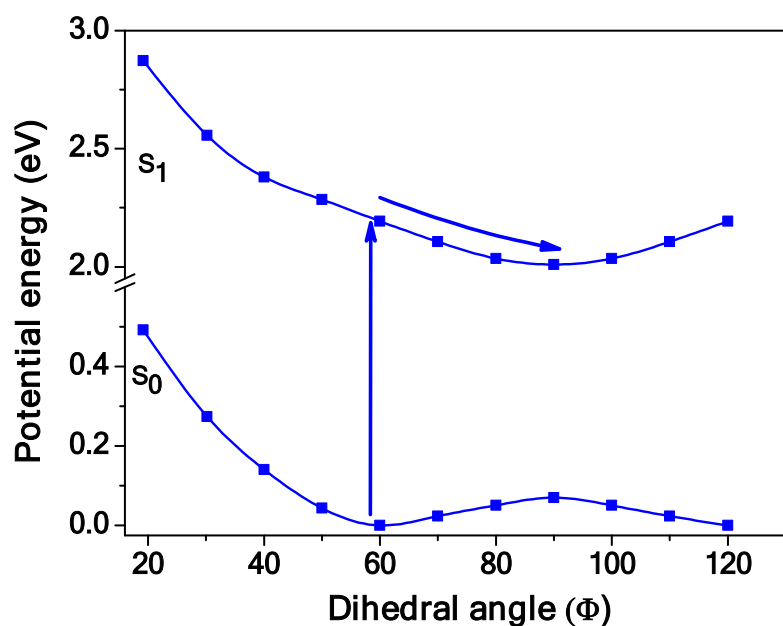


**Figure 9:** (A) Changes in potential energy of AnBTH<sup>+</sup> in S<sub>0</sub> and S<sub>1</sub> state as a function of dihedral angle between AN and BT units under rigid scan (i.e., other internal coordinates kept fixed). HOMO-LUMO composition of protonated AnBT at ground state (B) and excited state (C) geometry. Calculations were carried out in acetonitrile using polarizability continuum model.

1  
2 Calculation of potential energy (PE) of protonated AnBT shows interesting result. As  
3 shown in Figure 8A, PE of  $S_1$  state gradually decreases as we increase the dihedral angle and  
4 attains minimum at perpendicular geometry. Geometry optimization confirms that PE minima  
5 in  $S_1$  state of AnBTH<sup>+</sup> is located at perpendicular conformation (Dihedral angle between AN  
6 and BT is 89°). At this geometry, HOMO and LUMO molecular orbitals are completely  
7 localized at AN and BT units, respectively, decoupling orbitals of AN and BT and thus  
8 complete charge transfer at TICT geometry is attained. Calculated oscillator strength of  $S_0 \leftrightarrow S_1$   
9 transition of ground state ( $f \sim 0.29$ ) and excited state ( $f \sim 0.002$ ) optimized geometry supports  
10 relaxation to optically dark twisted state inferred from TA dynamics. In addition, low value of  
11 calculated  $S_0 \leftarrow S_1$  transition energy (1.8 eV) of twisted state of AnBTH<sup>+</sup> also supports fast  
12 deactivation to ground state in a few 100 ps timescale measured by TA spectroscopy.  
13  
14  
15  
16  
17  
18  
19  
20  
21

#### 22 4. Conclusion:

23  
24 In summary, we show that ultrafast dynamic planarization in picosecond timescale facilitates  
25 excitation delocalization in AnBT bichromophore. In absence of significant intramolecular  
26 charge transfer, conformational planarization dynamics in neutral AnBT appears to be  
27 diffusion controlled as revealed from viscosity dependence of picosecond relaxation  
28 component. On protonation, excited state conformational relaxation dynamics dramatically  
29 change. While planarization of chromophores in neutral AnBT leads to long lived emissive  $S_1$   
30 excited state, protonation of BT switches on picosecond nonradiative relaxation to a dark  
31 intermediate state by mutual twisting of AN and BT units. Protonation switches the direction  
32 of conformational motion from planarization to perpendicular direction. The concept of  
33 protonation induced intramolecular charge transfer driven torsional dynamics, previously  
34 proposed from quantum chemical calculation in donor acceptor chromophore<sup>55</sup> gains  
35 experimental validation in this study. Protonation induced alteration of excited state  
36 conformational motion and consequent effect on photophysical parameters may have  
37 implication in molecular motor and molecular switching applications.  
38  
39  
40  
41  
42  
43  
44  
45  
46  
47  
48

#### 49 SUPPORTING INFORMATION

50  
51  
52 *Supplementary photophysical data and ultrafast transient spectroscopic data are available in*  
53 *supporting information section.*  
54  
55

#### 56 AUTHOR INFORMATION

57 \*Corresponding author: Dr. Rajib Ghosh, E-mail: [rajchem06@gmail.com](mailto:rajchem06@gmail.com), [rajib@barc.gov.in](mailto:rajib@barc.gov.in)

58 **Note:** Authors declare no competing financial interest.  
59  
60

## ACKNOWLEDGEMENT

Funding from Department of Atomic Energy, India is gratefully acknowledged. D.D. gratefully acknowledges Department of Science and Technology for INSPIRE fellowship.

## REFERENCES

1. Kuang, Z.; He, G.; Song, H.; Wang, X.; Hu, Z.; Sun, H.; Wan, Y.; Guo, Q.; Xia, A.; Conformational Relaxation and Thermally Activated Delayed Fluorescence in Anthraquinone-Based Intramolecular Charge-Transfer Compound, *J. Phys. Chem. C*, **2018**, *122*, 3727–3737.
2. Chen, W.; Chen, C. –L.; Zhang, Z.; Chen, Y. –A.; Chao, W. –C.; Su, J.; Tian, H.; Chou, P. –T.; Snapshotting the Excited-State Planarization of Chemically Locked N,N'-Disubstituted Dihydrodibenzo[a,c]phenazines, *J. Am. Chem. Soc.*, **2017**, *139*, 1636–1644.
3. Piontkowski, Z.; McCamant, D. W.; Excited-State Planarization in Donor–Bridge Dye Sensitizers: Phenylene versus Thiophene Bridges, *J. Am. Chem. Soc.*, **2018**, *140*, 11046–11057.
4. Sabatini, R. P.; Mark, M. F.; Mark, D. J.; Kryman, M. W.; Hill, J. E.; Brennessel, W. W.; Detty, M. R.; Eisenberg, R.; McCamant, D. W. A Comparative Study of the Photophysics of Phenyl, Thienyl, and Chalcogen Substituted Rhodamine Dyes. *Photochem. Photobiol. Sci.* **2016**, *15*, 1417–1432.
5. Spettel, K. E.; Damrauer, N. H. Exploiting Conformational Dynamics of Structurally Tuned Aryl-Substituted Terpyridyl Ruthenium(II) Complexes to Inhibit Charge Recombination in Dye-Sensitized Solar Cells. *J. Phys. Chem. C* **2016**, *120*, 10815–10829.
6. Meylemans, H. A.; Hewitt, J. T.; Abdelhaq, M.; Vallett, P. J.; Damrauer, N.H. Exploiting Conformational Dynamics to Facilitate Formation and Trapping of Electron-Transfer Photoproducts in Metal Complexes. *J. Am. Chem. Soc.* **2010**, *132*, 11464–11466.
7. Meylemans, H. A.; Damrauer, N. H.; Controlling Electron Transfer through the Manipulation of Structure and Ligand-Based Torsional Motions: A Computational Exploration of Ruthenium Donor–Acceptor Systems using Density Functional Theory, *Inorg. Chem.* **2009**, *48*, 11161-11175.

- 1
  - 2
  - 3
  - 4
  - 5
  - 6
  - 7
  - 8
  - 9
  - 10
  - 11
  - 12
  - 13
  - 14
  - 15
  - 16
  - 17
  - 18
  - 19
  - 20
  - 21
  - 22
  - 23
  - 24
  - 25
  - 26
  - 27
  - 28
  - 29
  - 30
  - 31
  - 32
  - 33
  - 34
  - 35
  - 36
  - 37
  - 38
  - 39
  - 40
  - 41
  - 42
  - 43
  - 44
  - 45
  - 46
  - 47
  - 48
  - 49
  - 50
  - 51
  - 52
  - 53
  - 54
  - 55
  - 56
  - 57
  - 58
  - 59
  - 60
8. Ghosh, S.; Roscioli, J. D.; Bishop, M. M.; Gurchiek, J. S.; LaFountain, A. M.; Frank, H. A.; Beck, W. F.; Torsional Dynamics and Intramolecular Charge Transfer in the  $S_2$  ( $1^1B_u^+$ ) Excited State of Peridinin: A Mechanism for Enhanced Mid-Visible Light Harvesting, *J. Phys. Chem. Lett.*, **2016**, *7*, 3621–3626.
9. Nelson, T.; Fernandez-Alberti, S.; Roitberg, A. E.; Tretiak, S.; Electronic Delocalization, Vibrational Dynamics, and Energy Transfer in Organic Chromophores, *J. Phys. Chem. Lett.*, **2017**, *8*, 3020–3031.
10. Kim, P.; Park, K. H.; Kim, W.; Tamachi, T.; Iyoda, M.; Kim, D.; Relationship between Dynamic Planarization Processes and Exciton Delocalization in Cyclic Oligothiophenes, *J. Phys. Chem. Lett.* **2015**, *6*, 451-456.
11. Banerji, N.; Sub-picosecond Delocalization in the Excited State of Conjugated Homopolymers and Donor–Acceptor Copolymers, *J. Mater. Chem. C*, **2013**, *1*, 3052-3066.
12. Banerji, N.; Cowan, S., Vauthey, E. & Heeger, A. J.; Ultrafast Relaxation of the Poly (3-Hexylthiophene) Emission Spectrum. *J. Phys. Chem. C*, **2011**, *115*, 9726–9739.
13. Roy, P.; Jha, A.; Yasarapudi, V. B.; Ram, T.; Puttaraju, B.; Patil, S.; Dasgupta, J.; Ultrafast Bridge Planarization in Donor- $\pi$ -Acceptor Copolymers Drives Intramolecular Charge Transfer, *Nat. Comm.* **2017**, *8*, 1716.
14. Hintschich, S. I.; Dias, F. B.; Monkman, A. P.; Dynamics of Conformational Relaxation in Photoexcited Oligofluorenes and Polyfluorene, *Phys. Rev. B*, **2006**, *74*, 045210.
15. Dias, F. B.; Maçanita, A. L.; Melo, J. X.; Burrows, H. D.; Güntner, R.; Scherf, U.; Monkman, A. P.; Picosecond Conformational Relaxation of Singlet Excited Polyfluorene in Solution, *J. Chem. Phys.* **2003**, *118*, 7119.
16. Park, K. H.; Kim, W.; Yang, J.; Kim, D.; Excited-State Structural Relaxation and Exciton Delocalization Dynamics in Linear and Cyclic  $\pi$ -Conjugated Oligothiophenes, *Chem. Soc. Rev.*, **2018**, *47*, 4279-4294.
17. Park, K. H.; Kim, P.; Kim, J.; Shimizu, H.; Han, M.; Sim, E.; Iyoda, M.; Kim, D.; Excited-State Dynamic Planarization of Cyclic Oligothiophenes in the Vicinity of a Ring-to-Linear Excitonic Behavioral Turning Point, *Angew. Chem. Int. Ed.* **2015**, *54*, 12711-12715.
18. Zhou, J.; Yu, W.; Bragg, A. E.; Structural Relaxation of Photoexcited Quaterthiophenes Probed with Vibrational Specificity, *J. Phys. Chem. Lett.*, **2015**, *6*, 3496–3502.
19. Richert, S.; Limburg, B.; Anderson, H. L.; Timmel, C. R.; On the Influence of the Bridge on Triplet State Delocalization in Linear Porphyrin Oligomers, *J. Am. Chem. Soc.*, **2017**, *139*, 12003–12008.

- 1
  - 2
  - 3
  - 4
  - 5
  - 6
  - 7
  - 8
  - 9
  - 10
  - 11
  - 12
  - 13
  - 14
  - 15
  - 16
  - 17
  - 18
  - 19
  - 20
  - 21
  - 22
  - 23
  - 24
  - 25
  - 26
  - 27
  - 28
  - 29
  - 30
  - 31
  - 32
  - 33
  - 34
  - 35
  - 36
  - 37
  - 38
  - 39
  - 40
  - 41
  - 42
  - 43
  - 44
  - 45
  - 46
  - 47
  - 48
  - 49
  - 50
  - 51
  - 52
  - 53
  - 54
  - 55
  - 56
  - 57
  - 58
  - 59
  - 60
20. Grabowski, Z. R.; Rotkiewicz, K.; Rettig, W. Structural Changes Accompanying Intramolecular Electron Transfer: Focus on Twisted Intramolecular Charge-Transfer States and Structures. *Chem. Rev.* **2003**, *103*, 3899-4032.
21. Sasaki, S.; Drummen, G. P. C.; Konishi, G. Recent Advances in Twisted Intramolecular Charge Transfer (TICT) Fluorescence and Related Phenomena in Materials Chemistry, *J. Mater. Chem. C*, **2016**, *4*, 2731-2743.
22. Haidekker, M. A.; Theodorakis, E. A., Environment-Sensitive Behavior of Fluorescent Molecular Rotors. *J. Biol. Engin.* **2010**, *4*, 11.
23. Kuimova, M. K.; Yahioglu, G.; Levitt, J. A.; Molecular Rotor Measures Viscosity of Live Cells via Fluorescence Lifetime Imaging. *J. Am. Chem. Soc.* **2008**, *130*, 6672–6673.
24. Haidekker, M. A.; Lichlyter, D.; Johnny, M. B.; Grimes, C. A. Probing Polymerization Dynamics with Fluorescent Molecular Rotors and Magnetoelastic Sensors. *Sensor Lett.* **2006**, *4*, 257-261.
25. Lee, S. -C.; Heo, J.; Woo, H. C.; Lee, J. -A.; Seo, Y. H.; Lee, C. -L.; Kim, S.; Kwon, O. -P.; Fluorescent Molecular Rotors for Viscosity Sensor, *Chem. Euro. J.* **2018**, *24*, 13706-13718.
26. Duran, M.; Canbaz, M. C.; pKa Determination of Newly Synthesized N-(benzothiazole-2-yl)-2-(4,5-dimethyl-1-(phenylamino)-1H-imidazol-2-ylthio)acetamide Derivatives, *Ind. Eng. Chem. Res.* **2013**, *52*, 8355–8360.
27. Fayed, T. A.; Ali, S. S.; Protonation Dependent Photoinduced Intramolecular Charge Transfer in 2-(p-Dimethylaminostyryl) Benzazoles, *Spectro. Lett.* **2003**, *36*, 375-386.
28. Hrobáriková, V.; Hrobárik, P.; Gajdoš, P.; Fitis, I, Fakis, M.; Persephonis, P.; Zahradník, P.; Benzothiazole-Based Fluorophores of Donor- $\pi$ -Acceptor- $\pi$ -Donor Type Displaying High Two-Photon Absorption, *J. Org. Chem.*, **2010**, *75*, 3053–3068.
29. Hrobárik, P.; Hrobáriková, V.; Sigmundová, I.; Zahradník, P.; Fakis, M.; Polyzos, I.; Persephonis, P.; Benzothiazoles with Tunable Electron-Withdrawing Strength and Reverse Polarity: A Route to Triphenylamine-Based Chromophores with Enhanced Two-Photon Absorption, *J. Org. Chem.*, **2011**, *76*, 8726–8736.
30. Wang, X.; a Yang, J.; Yu, H.; Li, F.; Fan, L.; Sun, W.; Liu, Y.; Koh, Z. Y.; Pan, J.; Yim, W. -L.; Yan, L.; Wang, Q.; A Benzothiazole-Cyclopentadithiophene Bridged D-A- $\pi$ -A Sensitizer with Enhanced Light Absorption for High Efficiency Dye-Sensitized Solar Cells, *Chem. Commun.*, **2014**, *50*, 3965-3968.
31. Horiuchi, T.; Yashiro, T.; Kawamura, R.; Uchida, S.; Segawa, H.; Indoline Dyes with Benzothiazole Unit for Dye-sensitized Solar Cells. *Chem. Lett.* **2016**, *30*, 10.1246/cl.160084.

- 1  
2  
3  
4  
5  
6  
7  
8  
9  
10  
11  
12  
13  
14  
15  
16  
17  
18  
19  
20  
21  
22  
23  
24  
25  
26  
27  
28  
29  
30  
31  
32  
33  
34  
35  
36  
37  
38  
39  
40  
41  
42  
43  
44  
45  
46  
47  
48  
49  
50  
51  
52  
53  
54  
55  
56  
57  
58  
59  
60
32. Liu, H.; Zhuang, H.; Li, H.; Lu, J.; Wang, L.; Electronic Effect of Terminal Acceptor Groups on Different Organic Donor–Acceptor Small-Molecule Based Memory Devices, *Phys. Chem. Chem. Phys.*, **2014**, *16*,17125.
33. Ghosh, R. Nandi, A.; Palit, D. K. Solvent Sensitive Intramolecular Charge Transfer Dynamics in the Excited States of 4-N,N-Dimethylamino-4'-Nitrobiphenyl, *Phys. Chem. Chem. Phys.*, **2016**,*18*, 7661-7671.
34. Slavov, C.; Hartmann, H.; Wachtveitl, J.; Implementation and Evaluation of Data Analysis Strategies for Time-Resolved Optical Spectroscopy, *Anal. Chem.* **2015**, *87*, 2328-2336.
35. Schmidt, M. W.; Baldrige, K. K.; Boatz, J. A.; Elbert, S. T.;Gordon, M. S.; Jensen, J. H.; Koseki, S.; Matsunaga, N.; Nguyen, K. A.;Su, S. J.; Windus, T. L.; Dupuis, M.; Montgomery, J. A.; General Atomic and Molecular Electronic Structure System, *J. Comput. Chem.***1993**, *14*, 1347-1363.
36. Sasaki, T.; Inoue, T.; Komori, Y.; Irie, S.; Sakurai, K.; Tsubakiyama, K.; Photophysics of Novel 2,6-Disubstituted Benzobisthiazoles Possessing Chromophoric Groups, *Phys. Chem. Chem. Phys.*, **2003**, *5*, 1381–1385
37. Jurczok, M.; Plaza, P.; Martin, M. M.; Meyer, Y. H.; Rettig, W.; Excited state relaxation paths in 9,9'-bianthryl and 9-carbazolyl-anthracene: a sub-ps transient absorption study, *Chem. Phys.* **2000**, *253*, 339-349.
38. Cirmi, G.; Brida, D.; Gambetta, A.; Piacenza, M.; Sala, F. D.; Favaretto, L.; Cerullo, G.; Lanzani, G.; Observation and control of coherent torsional dynamics in a quinquethiophene molecule, *Phys. Chem. Chem. Phys.*, **2010**, *12*, 7917-7923.
39. Verolet, Q.; Rosspeintner, A.; Soleimanpour, S.; Sakai, N.; Vauthey, E.; Matile, S.; Turn-On Sulfide  $\pi$  Donors: An Ultrafast Push for Twisted Mechanophores, *J. Am. Chem. Soc.* **2015**, *137*, 15644–15647.
40. Siebert, R.; Winter, A.; Schubert, U. S.; Dietzek, B.; Popp, Excited-State Planarization as Free Barrierless Motion in a  $\pi$ -Conjugated Terpyridine, *J. Phys. Chem. C*, **2010**, *114*, 6841–6848.
41. Heisler, I. A.; Kondo, M.; Meech, S. R.; Reactive Dynamics in Confined Liquids: Ultrafast Torsional Dynamics of Auramine O in Nanoconfined Water in Aerosol OT Reverse Micelles, *J. Phys. Chem. B* **2009**, *113*, 1623-1631.
42. Horng, M. L.; Gardecki, J. A.; Papazyan, A.; Maroncelli, M. Subpicosecond Measurements of Polar Solvation Dynamics: Coumarin 153 Revisited, *J. Phys. Chem.* **1995**, *99*, 17311-17337.

- 1  
2  
3  
4  
5  
6  
7  
8  
9  
10  
11  
12  
13  
14  
15  
16  
17  
18  
19  
20  
21  
22  
23  
24  
25  
26  
27  
28  
29  
30  
31  
32  
33  
34  
35  
36  
37  
38  
39  
40  
41  
42  
43  
44  
45  
46  
47  
48  
49  
50  
51  
52  
53  
54  
55  
56  
57  
58  
59  
60
43. Ghosh, R.; Palit, D. K. Ultrafast Twisting Dynamics of Thioflavin-T: Spectroscopy of the Twisted Intramolecular Charge-Transfer State, *ChemPhysChem*. **2014**, *15*, 4126-4131.
  44. Ghosh, R.; Kushwaha, A.; Das, D.; Conformational Control of Ultrafast Molecular Rotor Property: Tuning Viscosity Sensing Efficiency by Twist Angle Variation, *J. Phys. Chem. B*, **2017**, *12*, 8786-8794.
  45. Ghosh, R.; Palit, D. K.; Effect of Donor–Acceptor Coupling on TICT Dynamics in the Excited States of Two Dimethylamine Substituted Chalcones, *J. Phys. Chem. A*, **2015**, *119*, 11128–11137.
  46. Marcus, Y. *Properties of solvents*; Wiley: New York 1998.
  47. Tang, T.; Chi, H.; Lin, T.; Wang, F.; He, C.; Protonation Induced Shifting of Electron-Accepting Centers in Intramolecular Charge Transfer Chromophores: A Theoretical Study, *Phys. Chem. Chem. Phys.*, **2014**, *16*, 20221-20227.
  48. Felouat, A.; D’Aléo, A.; Charaf-Eddin, A.; Jacquemin, D.; Guennic, B. L.; Kim, E.; Lee, K. J.; Woo, J. H.; Ribierre, J. –C.; Wu, J. W.; Fages, F.; Tuning the Direction of Intramolecular Charge Transfer and the Nature of the Fluorescent State in a T-Shaped Molecular Dyad, *J. Phys. Chem. A*, **2015**, *119*, 6283–6295.
  49. Saha, S. K.; Purkayastha, P.; Das, A. B.; Photophysical Characterization and Effect of pH on the Twisted Intramolecular Charge Transfer Fluorescence of Trans-2-[4-(Dimethylamino)Styryl]Benzothiazole, *J. Photochem. Photobiol. A* **2008**, *195*, 368-377.
  50. Grunder, S.; McGrier, P. L.; Whalley, A. C.; Boyle, M. M.; Stern, C.; Stoddart, J. F.; A Water-Soluble pH-Triggered Molecular Switch, *J. Am. Chem. Soc.* **2013**, *135*, 17691–17694
  51. Schafer, L. V.; Groenhof, G.; Boggio-Pasqua, M.; Robb, M. A.; Grubmuller, H.; Chromophore Protonation State Controls Photoswitching of the Fluoroprotein asFP595, *PLoS Comp. Biol.* **2008**, *4*, e1000034.
  52. Dial, B. E.; Pellechia, P. J.; Smith, M. D.; Shimizu, K. D.; Proton Grease: An Acid Accelerated Molecular Rotor, *J. Am. Chem. Soc.*, **2012**, *134*, 3675–3678.
  53. Wang, L.; Xiao, Y.; Deng, L.; Activatable Rotor for Quantifying Lysosomal Viscosity in Living Cells. *J. Am. Chem. Soc.* **2013**, *135*, 2903–2906.
  54. Nandi, A.; Kushwaha, A.; Das, D.; Ghosh, R.; Protonation Induced Ultrafast Torsional Dynamics of Anthrylbenzimidazole : A pH Activated Molecular Rotor, *Phys. Chem. Chem. Phys.*, **2018**, *20*, 7014-7020.

- 1  
2 55. Zhao, G. -J; Han, K. -L.; pH-Controlled Twisted Intramolecular Charge Transfer  
3 (TICT) Excited State via Changing the Charge Transfer Direction, *Phys. Chem. Chem.*  
4 *Phys.*, **2010**, *12*, 8914-8918.  
5  
6  
7

8 **TOC graph**  
9

